



Research paper

UV–VIS–NIR luminescence properties of an intense 5d broadband sensitized $\text{Eu}_2\text{SiS}_4:\text{Er}^{3+}$ suitable for solar spectral converter

Gongguo Zhang*, Qiuyu Cui, Guodong Liu

Key Laboratory of Inorganic Chemistry in Universities of Shandong, Department of Chemistry and Chemical Engineering, Jining University, Qufu, Shandong 273155, China

ARTICLE INFO

Article history:

Received 5 March 2016

In final form 17 May 2016

Available online 18 May 2016

ABSTRACT

A novel broadband sensitized near-infrared emitting phosphor, $\text{Eu}_2\text{SiS}_4:\text{Er}^{3+}$, was developed as promising solar spectral converter for Si solar cells. $\text{Eu}_2\text{SiS}_4:\text{Er}^{3+}$ has broadband absorptions ranging from 250 nm to 550 nm which can efficiently facilitate the UV–green part of the solar photon flux spectrum and exhibits intense NIR emission of Er^{3+} , perfectly matching the maximum spectral response of Si solar cells. The NIR integrated emission intensity of $\text{Eu}_2\text{SiS}_4:0.02\text{Er}^{3+}$ is 6.14 times as intense as that of a dual-mode solar spectral converter $\text{CaLaGa}_3\text{S}_6\text{O}:0.01\text{Ce}^{3+}, 0.06\text{Pr}^{3+}$. These results demonstrate that $\text{Eu}_2\text{SiS}_4:\text{Er}^{3+}$ phosphor is a promising candidate used as solar spectral converter.

© 2016 Elsevier B.V. All rights reserved.

1. Introduction

It is well known that the spectral mismatch between the solar photon flux spectrum (prominent in the UV–Vis region) and the optimal spectral response of Si solar cells (~ 1000 nm) is one of the main reasons limiting the efficiency of Si solar cells [1]. The spectral modification through downconversion has been regarded as an effective route to improve the performance of Si solar cells [2]. Up to now, much work has been done to develop solar spectral converter. For $\text{RE}^{3+}-\text{Yb}^{3+}$ (RE = Tb, Pr, Tm, Ho and Nd) co-doped materials [3–7], the RE^{3+} ion has only narrow and weak excitation band in the UV–Vis region because of parity forbidden 4f–4f transitions. So, these kinds of solar spectral converters are still far from practical application. Recently, much attentions have been paid on broadband solar spectral converter through host sensitization [8] or codoping Eu^{2+} [9,10], Ce^{3+} [11,12] and Bi^{3+} [13,14] with allowed 4f–5d, $^1\text{S}_0-^3\text{P}_1$ transitions. Unfortunately, most of them still suffer from relative narrower excitation bandwidth. In addition, their excitation band mainly locate in the 200–500 nm region. So, the green–red light ($\lambda \geq 500$ nm) which is the most intensive part of the solar photon flux spectrum cannot be absorbed. Consequently, novel full-spectrum (200–600 nm) solar spectral converters with broader absorption bands and intense NIR emission would be desirable for enhancing the efficiency of Si solar cells.

In this paper, we have developed a novel broadband sensitized near-infrared emitting phosphor $\text{Eu}_2\text{SiS}_4:\text{Er}^{3+}$ under N_2/CS_2 reducing atmosphere by solid-state reaction. Although NIR photoluminescence properties of $\text{Eu}_2\text{SiS}_4:\text{Er}^{3+}$ has been reported [15], the

synthesis method is too complex and time-consuming, and the concentration-dependent emission intensity (986 nm) has not been studied. In this letter, $\text{Eu}_2\text{SiS}_4:\text{Er}^{3+}$ has broadband absorptions ranging from 250 nm to 550 nm, and exhibits intense NIR emission of Er^{3+} , perfectly matching the maximum spectral response of Si solar cells. The NIR integrated emission intensity of $\text{Eu}_2\text{SiS}_4:0.02\text{Er}^{3+}$ is 6.14 times as intense as that of a dual-mode solar spectral converter $\text{CaLaGa}_3\text{S}_6\text{O}:0.01\text{Ce}^{3+}, 0.06\text{Pr}^{3+}$ (CLGSO:0.01 $\text{Ce}^{3+}, 0.06\text{Pr}^{3+}$) [16]. We believe $\text{Eu}_2\text{SiS}_4:0.02\text{Er}^{3+}$ could be a promising luminescent material used as solar spectral converter.

2. Experimental

2.1. Synthesis of samples

All powder samples of $\text{Eu}_2\text{SiS}_4:\text{Er}^{3+}$ were synthesized by conventional solid-state reaction. EuS, and Er_2S_3 were prepared from Eu_2O_3 (99.99%), and Er_2O_3 (99%) under N_2/CS_2 reducing atmosphere at 1000 °C for 3 h, and 1200 °C for 6 h, respectively. The stoichiometric amounts of materials EuS, Si powder (Alfa Aesar, 99.9%), and Er_2S_3 were thoroughly mixed in an agate mortar, and then the mixture was transferred into crucibles and sintered at 950 °C for 6 h under flowing N_2/CS_2 gas in horizontal tube furnace. CLGSO:0.01 $\text{Ce}^{3+}, 0.06\text{Pr}^{3+}$ was prepared according to Ref. [16].

2.2. Characterization

The phase purity of the final samples was characterized by powder X-ray diffraction (XRD) on Bruker D8 advance X-ray diffractometer with Cu K α ($\lambda = 1.5405$ Å) radiation at 40 kV and 40 mA. The diffuse reflection spectra were recorded on a Varian Cary

* Corresponding author.

E-mail address: zlwjxs@163.com (G. Zhang).

5000 UV–Vis–NIR spectrophotometer equipped with double out-of-plane Littrow monochromator. The photoluminescence excitation (PLE) and photoluminescence (PL) spectra at room temperature were measured by FSP920-combined Time Resolved and Steady State Fluorescence Spectrometer (Edinburgh Instruments) equipped with a 450 W Xe lamp, TM300 excitation monochromator and double TM300 emission monochromators, thermo-electric cooled red sensitive PMT and R5509-72 NIR-PMT in a liquid nitrogen cooled housing (Hamamatsu Photonics K.K.). The spectral resolution for the steady measurements is about 0.05 nm in UV–VIS and about 0.075–0.01 nm in NIR.

3. Results and discussion

Fig. 1 shows the XRD patterns of the $\text{Eu}_2\text{Si}_4:\text{xEr}^{3+}$ ($x = 0, 0.004, 0.007, 0.01, 0.02, 0.04, 0.06$). The results indicate that all the diffraction peaks of samples can be indexed to a pure Eu_2Si_4 (JCPDS 70-4996). No other phase can be detected, indicating that the dopants have no obvious influence on the crystalline structure of the host. The lattice parameters of $\text{Eu}_2\text{Si}_4:\text{xEr}^{3+}$ ($x = 0.02, 0.04, 0.06$) with high concentration of Er^{3+} were calculated by MDI Jade 5.0 software. Table 1 shows the lattice parameters of Eu_2Si_4 [17] and $\text{Eu}_2\text{Si}_4:\text{xEr}^{3+}$ ($x = 0.02, 0.04, 0.06$). It is obviously seen that with the increasing concentration of Er^{3+} , the lattice parameters gradually decrease. It is consistent with the substitution of smaller Er^{3+} (effective ionic radius 0.89 Å for CN = 6) for Eu^{2+} (effective ionic radius 1.17 Å for CN = 6) [18]. The results confirm that Er^{3+} have incorporated into the Eu_2Si_4 host lattice.

High absorption efficiency is very important for luminescent materials. Fig. 2(a) shows the diffuse reflection and PLE spectra of $\text{Eu}_2\text{Si}_4:0.004\text{Er}^{3+}$. It is obvious that $\text{Eu}_2\text{Si}_4:0.004\text{Er}^{3+}$ shows an intense and wide absorption band in the range of 250–550 nm, ascribed to the host absorption, and a platform of diffuse reflectance in the wavelength range of 550–1200 nm. In addition, it should be noted that no sharp absorption peak of Er^{3+} is observed in the diffuse reflection and PLE spectra. The result is in agreement with that reported in the Ref. [15]. Therefore, intense NIR emission of $\text{Eu}_2\text{Si}_4:\text{Er}^{3+}$ should be expected because $\text{Eu}_2\text{Si}_4:\text{Er}^{3+}$ has an intense and wide absorption band in the range of 250–550 nm.

The PLE and NIR emission spectra of $\text{Eu}_2\text{Si}_4:0.004\text{Er}^{3+}$ are shown in Fig. 2(b). The PLE spectrum ($\lambda_{\text{em}} = 986$ nm) presents a broad band ranging from 250 nm to 550 nm. It is attributed to the $4f^7 \rightarrow 4f^65d^1$ transition of Eu^{2+} and consistent with the diffuse reflection spectrum (shown in Fig. 2). By comparing the NIR

emission spectrum of $\text{Eu}_2\text{Si}_4:0.004\text{Er}^{3+}$ ($\lambda_{\text{ex}} = 400$ nm) and the NIR emission spectrum of Eu_2Si_4 ($\lambda_{\text{ex}} = 400$ nm), the presence of the NIR emission of Er^{3+} (820 nm, 986 nm and 1150 nm) in the NIR emission spectrum of $\text{Eu}_2\text{Si}_4:0.004\text{Er}^{3+}$ suggests that the existence of energy transfer (ET) from Eu^{2+} to Er^{3+} . In addition, the existence of the $4f^7 \rightarrow 4f^65d^1$ transition of Eu^{2+} in the PLE spectrum of Er^{3+} ($\lambda_{\text{em}} = 986$ nm and $\lambda_{\text{em}} = 1150$ nm) also indicates that ET from Eu^{2+} to Er^{3+} occurs.

In order to optimize the NIR emission of the Er^{3+} ion, the concentration-dependent emission intensity of $\text{Eu}_2\text{Si}_4:\text{xEr}^{3+}$ was studied. Fig. 3(a) presents the NIR emission spectra of $\text{Eu}_2\text{Si}_4:\text{xEr}^{3+}$ ($x = 0, 0.004, 0.007, 0.01, 0.02, 0.04, 0.06$) ($\lambda_{\text{ex}} = 400$ nm) and Fig. 3(b) exhibits the effects of the concentration of Er^{3+} on the NIR integrated emission intensity of Er^{3+} . It is obviously seen that with increasing Er^{3+} concentration, the NIR integrated emission intensity of Er^{3+} increases initially, then reaches a maximum at $x = 0.02$ and lastly decreases because of the concentration quenching.

Fig. 4 presents the energy level scheme of Eu^{2+} and Er^{3+} in Eu_2Si_4 , showing the NIR emission mechanism of $\text{Eu}_2\text{Si}_4:\text{Er}^{3+}$. As shown in Fig. 4, the energy difference between the lowest 5d excited level ($\sim 17,500$ cm^{-1}) of Eu^{2+} ion [15] and the $^4\text{F}_{9/2}$ level ($\sim 15,200$ cm^{-1}) of Er^{3+} ion is about 2300 cm^{-1} . It was reported that the maximum vibration frequency for thiosilicate is ~ 630 cm^{-1} [19]. Therefore, it is reasonable that ET occurs from the lowest 5d excited level of Eu^{2+} ion to the $^4\text{F}_{9/2}$ level of Er^{3+} ion by assistance of about 3–4 phonons. After the $^4\text{F}_{9/2}$, $^4\text{I}_{9/2}$, and $^4\text{I}_{11/2}$ levels are populated via ET and non-radiative relaxation, the NIR emission centering at 820 nm, 986 nm, and 1150 nm can be obtained, ascribed to the $^4\text{I}_{9/2} \rightarrow ^4\text{I}_{15/2}$, $^4\text{I}_{11/2} \rightarrow ^4\text{I}_{15/2}$, and $^4\text{F}_{9/2} \rightarrow ^4\text{I}_{13/2}$ transitions, respectively.

As an ideal solar spectral converter, it should convert visible photons into ~ 1000 nm photons, perfectly matching the maximum spectral response of Si solar cells. Fig. 5 shows spectra of $\text{Eu}_2\text{Si}_4:0.02\text{Er}^{3+}$ and CLGSO:0.01 Ce^{3+} , 0.06 Pr^{3+} , the solar photon flux spectrum and the spectral response of c-Si. CLGSO:0.01 Ce^{3+} , 0.06 Pr^{3+} is a promising dual-mode spectral-converting material. As shown in Fig. 5, $\text{Eu}_2\text{Si}_4:0.02\text{Er}^{3+}$ has intense wide excitation band extending from 250 to 550 nm. Table 2 shows the spectral properties of $\text{Eu}_2\text{Si}_4:\text{Er}^{3+}$ and previously reported solar spectral converter [8–14]. It is obviously seen that the main absorption bands in previously reported solar spectral converter are mostly less than 500 nm. Comparatively, $\text{Eu}_2\text{Si}_4:\text{Er}^{3+}$ has a broader absorption band (250–550 nm). The broad excitation bandwidth was desirable in practical application because more high-energy photons in the strongest region of the solar photon flux spectrum can be converted into NIR photons. Moreover, $\text{Eu}_2\text{Si}_4:0.02\text{Er}^{3+}$ has intense NIR emissions centering at 986 nm and 1150 nm. Under 400 nm excitation, the NIR integrated emission intensity of $\text{Eu}_2\text{Si}_4:0.02\text{Er}^{3+}$ is 6.14 times that of CLGSO:0.01 Ce^{3+} , 0.06 Pr^{3+} . These results demonstrate that $\text{Eu}_2\text{Si}_4:\text{Er}^{3+}$ phosphor is a promising candidate for enhancing the performance of Si solar cells. In the future, it should be combined with Si solar cell in order to give evidence on the extent to which the performance of Si solar cell will be improved. The solar spectral converter should be located on the front surface of Si solar cell in the experiment, and it is electrically isolated from the Si solar cell. The incident high-energy photons in the UV–Vis region (250–550 nm) can be absorbed and converted into NIR photons (~ 1000 nm) by the solar spectral converter, then the converted NIR photons can be effectively absorbed by Si solar cell. The charge thermalization of Si solar cell generated by the absorption of high-energy photons will be greatly decreased. This results in an increased spectral response of Si solar cell in UV–Vis spectrum region. Consequently, the performance of Si solar cell will be improved. Therefore, from the viewpoint of

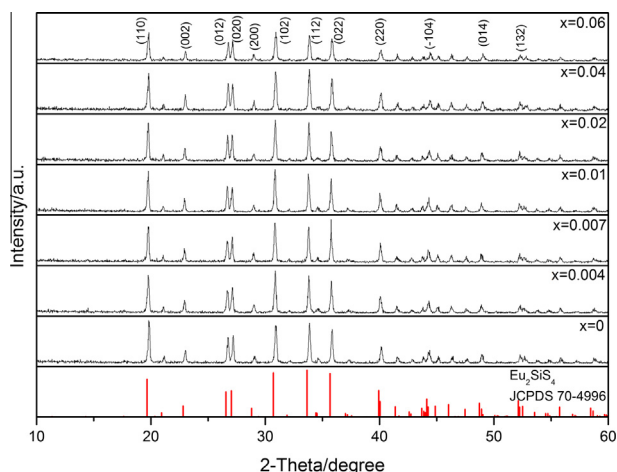


Fig. 1. Powder XRD patterns of $\text{Eu}_2\text{Si}_4:\text{xEr}^{3+}$ ($x = 0, 0.004, 0.007, 0.01, 0.02, 0.04, 0.06$).

Table 1
The lattice parameters of Eu_2Si_4 [17] and $\text{Eu}_2\text{Si}_4:\text{xEr}^{3+}$ ($x = 0.02, 0.04, 0.06$).

Lattice parameters	Eu_2Si_4 [17]	$\text{Eu}_2\text{Si}_4:0.02\text{Er}^{3+}$	$\text{Eu}_2\text{Si}_4:0.04\text{Er}^{3+}$	$\text{Eu}_2\text{Si}_4:0.06\text{Er}^{3+}$
a (Å)	6.524	6.518	6.507	6.494
b (Å)	6.591	6.584	6.583	6.576
c (Å)	8.205	8.177	8.171	8.153
V (Å ³)	334.99	332.93	331.78	330.59

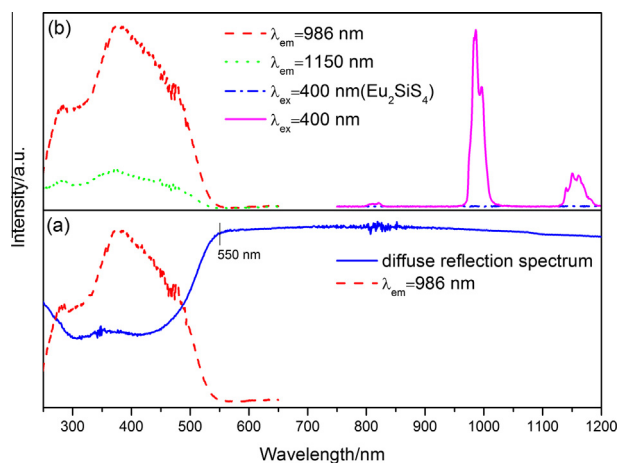


Fig. 2. (a) The diffuse reflection and PLE spectra of $\text{Eu}_2\text{Si}_4:0.004\text{Er}^{3+}$; (b) PLE and NIR emission spectra of $\text{Eu}_2\text{Si}_4:0.004\text{Er}^{3+}$.

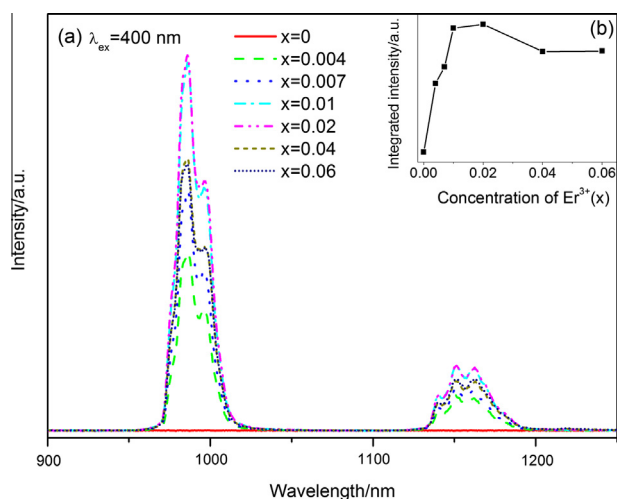


Fig. 3. (a) The NIR emission spectra of $\text{Eu}_2\text{Si}_4:\text{xEr}^{3+}$ ($x = 0, 0.004, 0.007, 0.01, 0.02, 0.04, 0.06$) ($\lambda_{\text{ex}} = 400$ nm); (b) the inset shows the NIR integrated emission intensity of Er^{3+} as a function of Er^{3+} concentration.

spectral characteristics, $\text{Eu}_2\text{Si}_4:\text{Er}^{3+}$ could be a promising luminescent material used as solar spectral converter.

4. Conclusions

To summarize, a novel broadband sensitized near-infrared emitting phosphor, $\text{Eu}_2\text{Si}_4:\text{Er}^{3+}$, was developed as promising solar spectral converter for Si solar cells. It has broadband absorptions ranging from 250 nm to 550 nm, and exhibits intense NIR emission of Er^{3+} , perfectly matching the maximum spectral response of Si solar cells. The NIR integrated emission intensity of $\text{Eu}_2\text{Si}_4:0.02\text{Er}^{3+}$ is 6.14 times as intense as that of a dual-mode

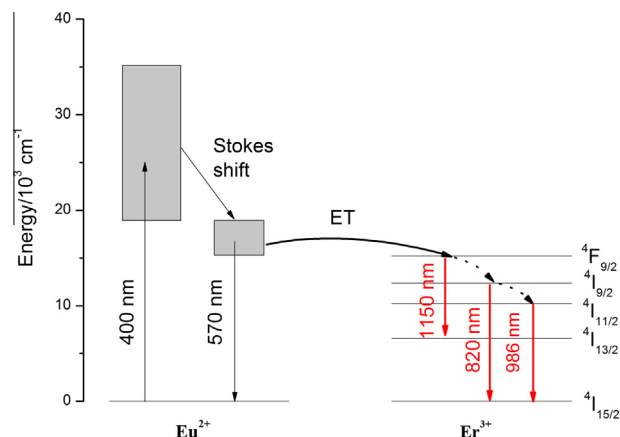


Fig. 4. Energy level scheme of Eu^{2+} and Er^{3+} in Eu_2Si_4 , showing the NIR emission mechanism of $\text{Eu}_2\text{Si}_4:\text{Er}^{3+}$.

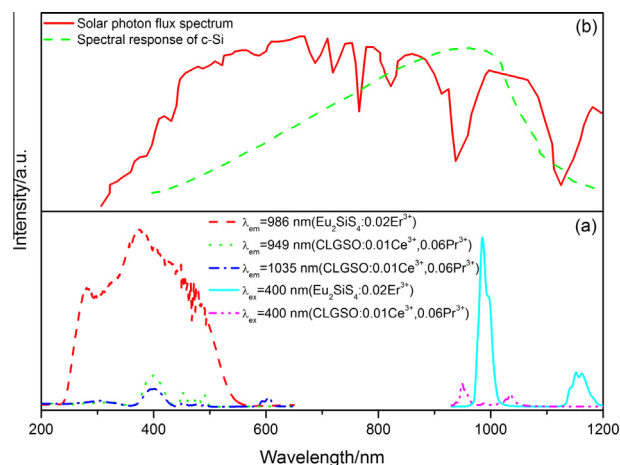


Fig. 5. (a) Spectra of $\text{Eu}_2\text{Si}_4:0.02\text{Er}^{3+}$ and $\text{CLGSO}:0.01\text{Ce}^{3+}, 0.06\text{Pr}^{3+}$, (b) solar photon flux spectrum, spectral response of c-Si.

Table 2
PLE and PL of different solar spectral converters.

Solar spectral converter	Excitation band (nm)	Emission (nm)	Reference
$\text{BaGd}_2(\text{MoO}_4)_4:\text{Yb}^{3+}$	260–375	1000	[8]
$\text{SrAl}_2\text{O}_4:\text{Eu}^{2+}, \text{Yb}^{3+}$	260–420	980	[9]
$\text{Sr}_2\text{Gd}(\text{PO}_4)_3:\text{Eu}^{2+}, \text{Yb}^{3+}$	280–440	975	[10]
$\text{LSCAS}:\text{Ce}^{3+}, \text{Yb}^{3+}$	375–500	980	[11]
$\text{Y}_3\text{Al}_5\text{O}_{12}:\text{Ce}^{3+}, \text{Nd}^{3+}$	300–525	1064	[12]
$\text{YVO}_4:\text{Bi}^{3+}, \text{Yb}^{3+}$	280–370	1039	[13]
$\text{Gd}_2\text{O}_3:\text{Bi}^{3+}, \text{Yb}^{3+}$	300–400	977	[14]
$\text{Eu}_2\text{Si}_4:\text{Er}^{3+}$	250–550	986	This work

solar spectral converter $\text{CLGSO}:0.01\text{Ce}^{3+}, 0.06\text{Pr}^{3+}$. We believe $\text{Eu}_2\text{Si}_4:\text{Er}^{3+}$ could be a promising luminescent material used as solar spectral converter.

Acknowledgments

This work was supported by the Research Foundation for Excellent Young and Middle-Aged Scientists of Shandong Province (BS2013CL027), the High Educational Science & Research Foundation of Shandong Province (J14LC18) and the National Undergraduate Innovation and Entrepreneurship Training Program (201510454006).

References

- [1] B.S. Richards, *Sol. Energy Mater. Sol. Cells* 90 (2006) 2329.
- [2] T. Trupke, M.A. Green, P. Würfel, *J. Appl. Phys.* 92 (2002) 1668.
- [3] W.X. Bai, Y.H. Liu, Y.P. Wang, X.H. Qiang, L.B. Feng, *Ceram. Int.* 41 (2015) 12896.
- [4] B.M. van der Ende, L. Aarts, A. Meijerink, *Adv. Mater.* 21 (2009) 1.
- [5] F. Huang, L.Y. Chen, Y. Han, J.Z. Tang, Q.H. Nie, P.Q. Zhang, Y.S. Xu, *Infrared Phys. Technol.* 71 (2015) 159.
- [6] K.M. Deng, T. Gong, L.X. Hu, X.T. Wei, Y.H. Chen, M. Yin, *Opt. Express* 19 (2011) 1749.
- [7] D.Q. Chen, Y.L. Yu, H. Lin, P. Huang, Z.F. Shan, Y.S. Wang, *Opt. Lett.* 35 (2010) 220.
- [8] Y. Guan, L. Qin, Y.L. Huang, T.J. Tsuboi, W. Huang, *Mater. Lett.* 117 (2014) 4.
- [9] Y.P. Tai, G.J. Zheng, H. Wang, J.T. Bai, *J. Solid State Chem.* 226 (2015) 250.
- [10] J.Y. Sun, Y.N. Sun, J.H. Zeng, H.Y. Du, *Opt. Mater.* 35 (2013) 1276.
- [11] Z.J. Liu, J.Y. Li, L.Y. Yang, Q.Q. Chen, Y.B. Chu, N.L. Dai, *Sol. Energy Mater. Sol. Cells* 122 (2014) 46.
- [12] Y.P. Tai, G.J. Zheng, H. Wang, J.T. Bai, *J. Photochem. Photobiol. A* 303–304 (2015) 80.
- [13] U. Rambabu, S.-D. Han, *Ceram. Int.* 39 (2013) 1603.
- [14] X.Y. Huang, Q.Y. Zhang, *J. Appl. Phys.* 107 (2010) 063505.
- [15] M. Sugiyama, Y. Nanai, Y. Okada, T. Okuno, *J. Phys. D: Appl. Phys.* 44 (2011) 095404.
- [16] G.G. Zhang, C.M. Liu, J. Wang, X.J. Kuang, Q. Su, *J. Mater. Chem.* 22 (2012) 2226.
- [17] D. Johrendt, R. Pocha, *Acta Cryst. E57* (2001) i57.
- [18] R.D. Shannon, *Acta Cryst. A32* (1976) 751.
- [19] C. Köster, A. Lindemann, J. Kuchinke, C. Mück-Lichtenfeld, B. Krebs, *Solid State Sci.* 4 (2002) 641.